

Physical chemical properties of geomaterials

Ionov A.M.¹, Barkalov O.I.¹, Shulyatev D.A.², Gavrilicheva K.A.¹ and Shahlevich O.F.¹ Charoite transformations under thermal treatment

¹Osipyan Institute of Solid State Physics of the Russian Academy of Sciences, Chernogolovka, Russia (xenia.gavrilicheva@yandex.ru) ² Materials Modeling and Development Laboratory, NUST MISIS, Leninskiy prospect, 4, 199049 Moscow, Russia

Abstract Structural phase transformations of the charoite mineral induced by thermal treatment at high temperatures were studied by simultaneous monitoring of the thermogravimetry, differential scanning calorimetry, and mass spectrometry curves up and above to its melting temperature range (~ 1300 °C). The chemical composition and phase state of the initial and melted samples were characterized using electron-probe micro-analysis, X-ray powder diffraction, and Raman spectroscopy. It was demonstrated that continuous heating (10 °C/min) up to ~ 600 °C resulting in a mass loss of ~ 5 wt. % was due to crystallization water release and dehydroxylation, while oxygen release and carbonate inclusion decomposition were observed at a higher temperature. The endothermic peak with a heat effect of 82 J/g at 970 ÷ 1050 °C was attributed to the charoite-to-wollastonite transition detected by X-ray powder diffraction in this temperature range. Above 1100 °C, another extended endothermic effect was fixed, which was presumably due to the formation of pseudowollastonite and pre-melting processes. The melting of the charoite sample using the floating zone technique resulted in its transformation to pseudowollastonite and caused a significant color change from lilac to rose pink.

Keywords: charoite, thermogravimetry, calorimetry, X-ray diffraction, Raman spectroscopy, floating zone melting

Introduction. Charoite the so-called “lilac miracle of Siberia” is a delightful gemstone (Rogova et al. 2013). This mineral is well-known in the gem market due to its exciting aesthetic properties, such as unique lilac to violet color, structural features, and endemic origin. The main (Russian Federation, Murun massif) deposit “Sirenevyy Kamen” includes both charoite and charoite-containing rocks, with a idealized formula of $(K, Sr, Ba, Mn)_{15-16}(Ca, Na)_{32}[(Si_{70}(O, OH)_{180})](OH, F)_4 \cdot nH_2O$ (Rozhdestvenskaya et al. 2010), and a complex structure of alkaline calcium silicate with tubular Si-O-radicals: $(Ca_{1.57}Na_{0.51}K_{0.93}Ba_{0.07})_{3.11} \cdot Si_4O_{10}(OH_{0.58}F_{0.20})_{0.78} \cdot 0.72H_2O$ (Rogova et al. 2013). The chemical formula of charoite varies among different outcrops, with inclusions of aegirine, tinaksite, microcline, tokkoite and some other minerals of the metasomatic rocks also exhibits a complex association (Reguir 2001). The main charoite element components are K, Na, Ca, Si, and O, F, H₂O, OH, the secondary components are Ba,

Sr, and Mn; the presence of traceable amounts of Fe, Mg, Al, Ti, Zr, and Th is discovered in Murun charoite.

To understand the genesis and properties of charoite it is necessary to study the behavior of the mineral upon its heating to high temperatures up to the melting temperature. Moreover, the undoubted interest is to investigate the possibility of charoite crystallization during the melting process. Our study is focused on the high-temperature charoite behavior and the charoite transformation upon melting during crystallization.

Experimental methods and sample characterization. Experiments were conducted using high-quality samples of charoite mineral. To prepare samples for analysis and melting, samples 4x4x40 mm and 4x4x1 mm were cut from a mineral block of high jewelry quality, dark lilac-violet color, without visible white, black and yellow inclusions. The content of elements in charoite was determined at IPTM RAS by inductively coupled plasma atomic emission spectrometry (iCAP-6500, Thermo Scientific, USA) and mass spectral methods of analysis (X Series 2, Thermo Scientific, USA). The elemental composition of the samples was characterized before and after thermal treatment by scanning electron microscopy (SEM, Supra 50 VP with EDX detector, Carl Zeiss).

The Raman spectra were recorded with a Princeton Instruments HRS 500 spectrometer equipped with a liquid nitrogen-cooled charge-coupled device detector. The spectra were monitored with 1200 grooves/mm grating. The samples were irradiated at room temperature with a 532-nm KLM-532/SLN-100 DPSS (FTI Optronics, St. Petersburg, Russia) laser with a laser power at the sample of about 5 mW in a back-scattering geometry. A 20x Plan Apo Mitutoyo objective was used to focus the laser beam to a spot of approximately 3 μm in size and collect the scattered light. A razor edge Semrock beam splitter and a Holographic Tydex Notch-6 filter (Tydex, St. Petersburg, Russia) were used for laser line discrimination and acquiring the Raman spectra higher than 200 cm⁻¹. The spectral resolution in the spectral range under study was ≈ 1 cm⁻¹. The spectrometer was calibrated using Ne spectral lines with an uncertainty of ± 1 cm⁻¹.

The X-ray powder diffraction data (XRD) were taken on Rigaku SmartLab SE, Cu-Kα radiation, equipped with 1D D/teX PSD in Bragg-Brentano geometry (Cu-Kα_{1,2}, λ = 1.5418 Å) at room temperature. The data were collected in a 2θ range of 10-90° with a step of 0.01°.

Charoite transformations at high temperatures

were studied experimentally upon heating the samples from room temperature to 1300 °C in the air and argon atmosphere. NETZSCH STA 409 PC/PG was used for simultaneous thermogravimetric and calorimetric analyses from room temperature to a high-temperature of 1300 °C and allowed us to analyze the change in mass, to study the decomposition processes, thermal stability, and behavior during crystallization, and to determine enthalpy transitions, phase transition temperatures. The experiments were performed at a rate of

10.0 °C/min in an alumina crucible in argon.

Charoite rod were remelted by vertical non-crucible floating zone (FZ) melting with optical radiation heating (Balbashov and Egorov 1981).

Results. Charoite composition. The average chemical composition of the initial charoite sample was SiO₂=52.29%, CaO=31.42%, K₂O=7.60%, Na₂O=4.23%, BaO=2.50% (main components, total 98.04%, Supra 50, EDX detector). Element composition is summarized in Table 1.

Table1. Elemental composition of the charoite samples

	DL (ppm)	Lilac (iCAP-6500)	Lilac (X Series 2)	FZ Melted
Li	0.21	23.1	22.9	19.2
Be	0.21	21.5	16.1	7.18
B	0.79	385	300	<DL
Na	20	---	26000	19236
Mg	2.7	261	226	4.82
Al	200	674	123	21.4
Si	base	320000	309000	278050
K	6	---	48000	69315
Ca	450	190000	155000	158623
Sc	1.1	11.9	12.8	<DL
Ti	23	28.2	21.1	3.03
V	1.6	3.52	31.2	<DL
Cr	0.61	17.9	72.3	<DL
Fe	44	183	186	27.9
Mn	4.2	2709	2540	1904
Ni	0.34	9.51	9.66	0.43
Cu	0.65	69.9	101	7.07
Rb	0.03	330	306	288
Sr	0.06	8200	7660	23281
Y	0.04	100	80.4	71.2
Zr	0.23	46.7	40.7	36
Nb	0.02	4.82	4.05	3.38
Cs	0.02	23.7	18.8	16.9
Ba	0.48	36000	30400	38100
La	0.02	463	357	385
Ce	0.04	928	792	944
Pr	0.01	120	88.4	109
Nd	0.02	470	362	384
Sm	0.01	80.4	63.7	64.6
Eu	0.005	18.2	14.1	15.2
Gd	0.02	49.5	39.6	39.1
Tb	0.01	5.26	4.03	4.05
Dy	0.02	23.9	18.5	19.1
Er	0.01	8.19	6.31	6.66
Yb	0.01	4.75	3.69	3.99
W	0.02	7.72	6.49	0.038
Pb	2.6	64.1	36.5	19.8
U	0.01	18.9	14.1	22

DL – Detection limit

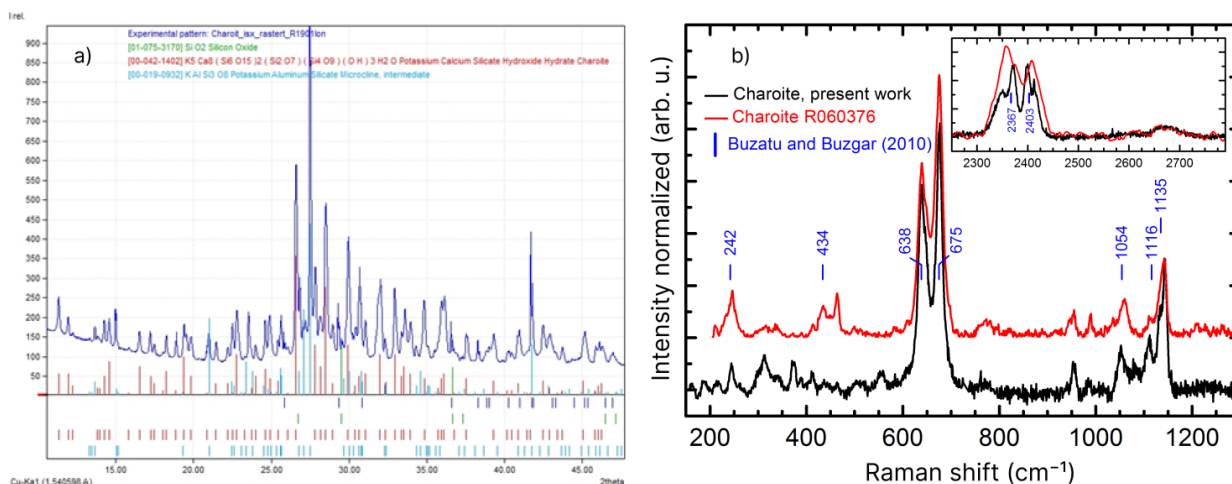


Fig. 1 The initial charoite sample: a) The blue curve is X-ray diffraction pattern (CuK α_1 radiation); b) The Raman spectrum of charoite: black - present work, red - RRUFF [R060376](#).

CHAROITE SPECTROSCOPY. The XRD powder pattern and Raman spectrum of the initial charoite sample are presented in Fig. 1 and agree well with the experimental data available in the literature (RRUFF Project database [R060376](#); Buzatu and Buzgar 2010; Rozhdestvenskaya et al. 2010).

Only a few studies were made on charoite (Rogova et al. 1978; Rozhdestvenskaya et al. 2009). The Raman spectra for charoite from the RRUFF (R060376) are similar to the spectrum obtained in the present study. No discussions or detailed vibration mode assignments for this mineral were found in the literature. The Raman spectrum of charoite (Fig. 1, right panel) is characterized by strong fluorescence and background, the peaks are very weak, and only a few of them can be resolved. The peak positions are very close to those reported in (Buzatu and Buzgar

2010). An intensive and broad band around 2400 cm $^{-1}$ is most probably of luminescence origin. It corresponds to the wavelength of ~ 610 nm, i.e., to the red region of the visible light spectrum.

THERMAL TREATMENT. The charoite transformation at high temperatures was studied by heating the samples from RT to 1300 °C in argon and the air. First, a charoite sample placed in the alumina or platinum crucibles was heated in the air in a furnace. After heating above 900 °C in the air, the violet color of charoite began to fade, and the sample melted above 1000 °C. These findings probably indicate that the structural transformations of charoite began above 900 °C and agree with the results of (Nikolskaya et al. 1976), where the charoite sample was discolored completely by annealing under the reducing conditions for three hours at 700 °C.

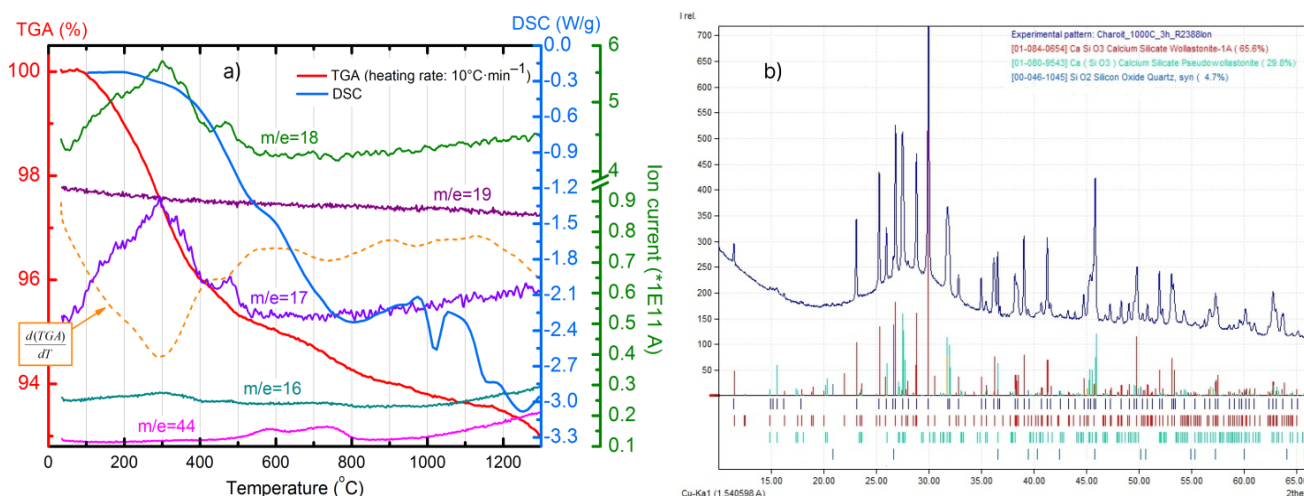


Fig. 2. a) DSC, TGA curves along with the mass spectrometric curves for the initial charoite sample. The dash curve represents the first derivative of the TGA curve; b) XRD pattern of charoite sample annealed at 1000 °C, 3 hours.

As demonstrated by the mass-spectral curves presented in Fig. 2a, upon heating, the water release ($m/e = 17, 18$) from the charoite sample occurred in a temperature range of $\sim 50\text{--}600$ °C, while the release of carbon dioxide ($m/e = 44$) proceeded at $500\text{--}800$ °C, and that of carbon dioxide and atomic oxygen occurred above ~ 1000 °C.

The thermogravimetric curve measured upon heating charoite shown in Fig. 2a demonstrates singularities at 208, 295, and 460 °C. These values are close to those of our mass spectrometry curves for water ($m/e = 18$) and hydroxyl group ($m/e = 17$), as shown in Fig. 2a, and those reported in (Matesanz et al. 2008) for the TGA and DTA dependencies. The DSC curve measured in the present work demonstrates a pronounced endothermic shift right above 200 °C and up to ~ 800 °C. It is featureless in this temperature range probably due to the overlapping of the dehydration, dehydroxylation, and carbonate decomposition processes. A deflection of the first derivative curve of the DSC signal between 500 and 560 °C might point to the peak position of the endothermic processes within this temperature range. The baseline of the DSC signal is more or less leveled above 800°C, and above 900°C two endothermic peaks are observed. The former narrow endothermic peak with the onset at ~ 990 °C and an enthalpy change of 82 J/g should be due to the charoite-to-wollastonite phase transition since the characteristic temperatures determined by the DSC method in the present work coincide with the temperatures obtained by the real-time XRD method and reported in (Janeczek 1991). The mediate sample annealed at 1000 °C for 3 hours is composed of free phases (see Fig. 2b). There are wollastonite (65.6%), pseudowollastonite (29.8%) and a small amount of quartz ($\sim 4.7\%$). We assume that the latter broad heat effect fixed above 1100 °C corresponds to the formation of pseudowollastonite from wollastonite and, probably, its premelting. According to the XRD phase analysis of the charoite samples subjected to isochronic annealing (Marchuk et al. 2016), the first traces of the pseudowollastonite phase appeared at ~ 1050 °C and a single phase state was attained at ~ 1250 °C. On the other hand, the synthetic wollastonite CaSiO_3 transforms to pseudowollastonite at 1180 °C (Allen et al. 1906). The melting point of the latter phase is 1512 °C (Allen et al. 1906) or 1547 °C (Richet et al. 1998). The endothermic process is obviously not finished at 1300 °C (see Fig. 2); thus, a calorimeter with a

higher temperature limit should be used to get a reliable DSC curve.

Hence, our direct mass-spectral and DSC/TGA experimental data confirm the assumptions on the dehydration and dehydroxylation of charoite upon heating. These assumptions were agreed with the results of DSC/TG and IR spectroscopy studies that were reported in (Janeczek 1991; Matesanz et al. 2008; Kaneva et al. 2020).

FLOATING ZONE MELTING. An attempt to grow a bulk polycrystalline sample of charoite is of undoubted interest, allowing for a reliable characterization of its physical properties and studying the high-temperature transformations of this mineral. Assuming that the growth of charoite crystals should apparently be carried out in a hydrothermal environment, in order to study the behavior of charoite under extreme thermal influences, attempts were made to grow a single crystal using non-crucible zone melting in an oxygen atmosphere. Non-crucible floating zone melting (FZM) with radiation heating is a suitable technique for growing high-quality complex oxide single crystals, as demonstrated in (Balbashov and Egorov 1981; Balbashev et al. 1996).

Charoite rod was remelted by vertical non-crucible floating zone (FZ) melting with optical radiation heating. Rods (4x4x40 mm) for FZ melting were prepared by cutting from the deep violet mineral block. The charoite rods were FZ melted in the air, the growth rate was $10\text{--}12$ mm/h at the beginning, and then 4mm/h. At end of melting 70 mm-long whisker was an easily retracted. As a result, the ingot in the form of cylindrical rods of $35\text{--}40$ mm in length and $3\text{--}4$ mm in diameter were obtained. The disk-shaped samples with a thickness of 1 mm and a diameter of 4 mm were prepared by cutting the grown cylindrical rods (see Fig. 3).

The sample color after melting and growth in the air is pale pink-lilac. According to the XRD, there are weak but rather amorphous reflections on the melted part, and the whisker is amorphous. The XRD powder pattern and Raman spectra from central part of ingot of the melted charoite minerals are presented in Fig.4.

The average chemical composition of the melted sample in the middle part (red line area) is $\text{SiO}_2=62.79\%$, $\text{CaO}=24.16\%$, $\text{K}_2\text{O}=4.28\%$, $\text{Na}_2\text{O}=8.76\%$ (main components, total 99.99%). Elemental composition is summarized in Table 2.

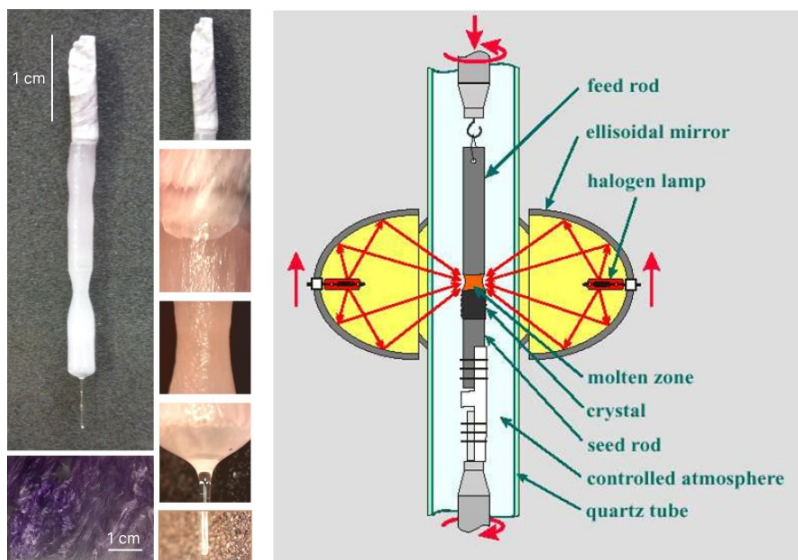


Fig.3 Left: photo of the polished charoite mineral block, the cylinder of charoite (about 40 mm in length and 4 mm in diameter) after melting. Right: non-crucible floating zone scheme.

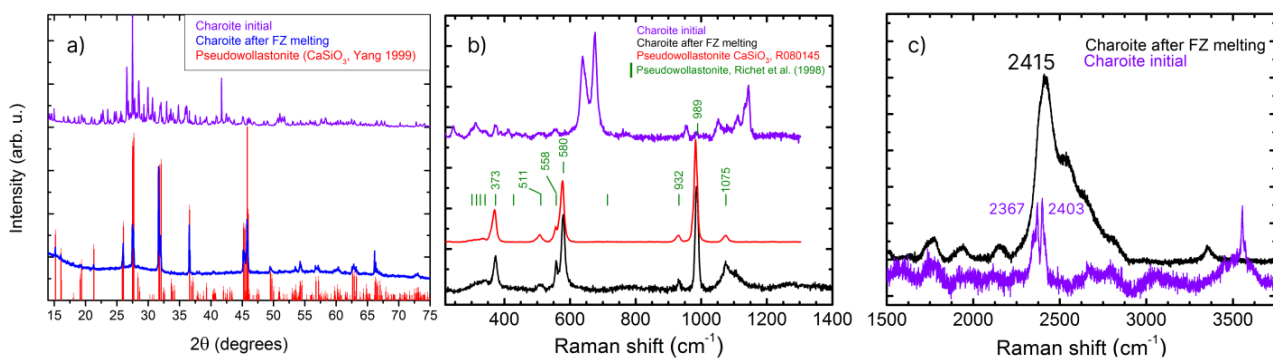


Fig.4. The charoite sample after FZ melting: a) The XRD pattern; b) the Raman spectra; c) the high-frequency part of the Raman spectra.

Table 2. Elemental composition of initial charoite and pseudowollastonite composite ingot melted by FZM

Sample melt	Precursor Charoite violet	Precursor Charoite violet	Thin end melted	Thin end melted	Centre melted	Centre melted	Thick end melted	Thick end melted
Element	Weight%	Atomic%	Weight%	Atomic%	Weight%	Atomic%	Weight%	Atomic%
O K	42.26	61.99	50.70	67.27	46.30	63.88	42.63	60.65
Na K	1.37	1.36	3.78	3.52	2.60	2.49	2.06	2.03
Si K	23.78	19.41	25.84	19.74	28.67	22.85	29.94	24.32
K K	6.45	3.78	7.66	4.32	9.80	5.56	10.22	5.94
Ca K	22.83	13.06	8.40	4.55	8.08	4.48	11.33	6.42
Ba L	2.31	0.39	3.62	0.60	4.55	0.74	3.82	0.64

Standard: O - SiO₂, Na - Albite, Si - SiO₂, K - MAD-10 Feldspar, Ca - Wollastonite, Ba -BaF₂.

Our XRD and Raman data (see Fig. 4) demonstrate the transformation of charoite to high-temperature modification called pseudowollastonite Ca(Na, K, Ba)SiO₃ having a pale pink color upon melting in the air (see also Table 2). An attempt to grow a single crystal of charoite by non-crucible floating zone (FZ) melting in an oxidizing atmosphere was unsuccessful due to the transformation of charoite into pseudowollastonite and its partial amorphization.

By using the tentative mode assignment made for

wollastonite by (Buzatu and Buzgar 2010) and for pseudowollastonite by (Richet et al. 1998), the following three frequency ranges might be distinguished in our Raman spectrum of the initial charoite sample and the pseudowollastonite phase (Fig. 4b, c) obtained by the FZ melting procedure. The first one below 500 cm⁻¹ corresponds to the metal-oxygen stretching modes, the second one, 500-850 cm⁻¹, refers to the O-Si-O bending and Si-O_{br} stretching vibrations, and the third one, 900-1180 cm⁻¹, corresponds to the SiO_{nbr} stretching vibrations.

However, in the high-frequency region, above 2300 cm^{-1} for charoite and above 1500 cm^{-1} for pseudowollastonite, a series of peaks is observed with a rather intensive broad band in a range of 2500–3000 cm^{-1} . The latter band is not an overtone of the low-frequency modes; thus, we assume it to be due to luminescence with a wavelength of ~ 610 nm, i.e., in the red region of the visible light spectrum.

Conclusions. By measuring simultaneously the weight loss (TGA), heat release (DSC), and mass spectrometry (MS) curves upon heating the charoite sample to 1300 °C, we found that the dehydration and dehydroxylation processes (water and hydroxyl group release, $m/e = 17, 18$) occurred at 50 – 460 °C. It should be noted that after dehydration and dehydroxylation (loss of 5 %) at 50 – 500 °C charoite structure still exist according XRD and Raman data. Carbon dioxide release ($m/e = 44$) observed in a temperature range of 500–800 °C was probably due to decomposition of the carbonate inclusion in the mineral, and the heated sample lost oxygen ($m/e = 16$) above 1000 °C. The endothermic peak monitored at 970 – 1055 °C with an integral enthalpy change of 82 J/g was due to the formation of wollastonite from charoite. The melting of charoite by the floating zone procedure resulted in its transition to a pseudowollastonite-like phase.

Acknowledgments

The authors would like to thank the Shared Facilities Center at the Osipyan Institute of Solid State Physics RAS (Chernogolovka) for the use of the micro-Raman optical system and Rigaku SmartLab SE diffractometer. This work was carried out within the framework of the Governmental Program of Osipyan Institute of Solid State Physics RAS.

References

- Allen ET, White WR, Wright FE (1906) On wollastonite and pseudo-wollastonite, polymorphic forms of calcium metasilicate, with optical study by F. E. Wright. *American Journal of Science* s4-21:89–108. <https://doi.org/10.2475/ajs.s4-21.122.89>
- Balbashev AM, Shulyatev DA, Panova GK, et al (1996) The floating zone growth and superconductive properties of $\text{La}_{1.85}\text{Sr}_{0.15}\text{CuO}_4$ and $\text{Nd}_{1.85}\text{Ce}_{0.15}\text{CuO}_4$ single crystals. *Physica C: Superconductivity* 256:371–377. [https://doi.org/10.1016/0921-4534\(95\)00647-8](https://doi.org/10.1016/0921-4534(95)00647-8)
- Balbashov AM, Egorov SK (1981) Apparatus for growth of single crystals of oxide compounds by floating zone melting with radiation heating. *Journal of Crystal Growth* 52:498–504. [https://doi.org/10.1016/0022-0248\(81\)90328-6](https://doi.org/10.1016/0022-0248(81)90328-6)
- Buzatu A, Buzgar N (2010) THE RAMAN STUDY OF SINGLE-CHAIN SILICATES. *Analele Stiintifice ale*

- Universitatii “Al I Cuza” din Iasi Seria Geologie LVI:107–125
- Janeczek J (1991) Thermal decomposition of charoite. *Mineralogia Polonica* 22:21–27
- Kaneva EV, Radomska TA, Shendrik RYu, et al (2020) FTIR, XRF and Powder XRD Experimental Study of Charoite: Crystal Chemical Features of Two Associated Generations. In: Votyakov S, Kiseleva D, Grokhovsky V, Shchapova Y (eds) *Minerals: Structure, Properties, Methods of Investigation*. Springer International Publishing, Cham, pp 97–104
- Marchuk MV, Medvedev VYa, Ivanova LA, et al (2016) CHAROITE. EXPERIMENTAL STUDIES. *Geodin tektonofiz* 7:105–118. <https://doi.org/10.5800/GT-2016-7-1-0199>
- Matesanz E, Garcia-Guinea J, Crespo-Feo E, et al (2008) THE HIGH-TEMPERATURE BEHAVIOR OF CHAROITE. *The Canadian Mineralogist* 46:1207–1213. <https://doi.org/10.3749/canmin.46.5.1207>
- Nikolskaya L, Novozhilov A, Samoilovich M (1976) On the nature of colours of the new alkaline calcium silicate from the Eastern Transbaikalia. *Izv AN SSSR* 116–120
- Richet P, Mysen BO, Ingrin J (1998) High-temperature X-ray diffraction and Raman spectroscopy of diopside and pseudowollastonite. *Physics and Chemistry of Minerals* 25:401–414. <https://doi.org/10.1007/s002690050130>
- Rogova V, Rogov Y, Drits V, Kuznetsova N (1978) Charoite — a new mineral, and a new jewelery stone. *Zapiski Vsesoyuznogo Mineralogicheskogo Obshchestva* 107:94–100.
- Rogova V, Rozhdestvenskaya I, Vorobjov E, et al (2013) Charoite. *The Lilac Miracle of Siberia*. Illustrated popular science book, 2nd edn. Petrografika, Irkutsk
- Rozhdestvenskaya I, Mugnaioli E, Czank M, et al (2010) The structure of charoite, $(\text{K},\text{Sr},\text{Ba},\text{Mn})_{15-16}(\text{Ca},\text{Na})_{32}[(\text{Si}_{70}(\text{O},\text{OH})_{180})](\text{OH},\text{F})_{4.0}\cdot n\text{H}_2\text{O}$, solved by conventional and automated electron diffraction. *Mineral mag* 74:159–177. <https://doi.org/10.1180/minmag.2010.074.1.159>
- Rozhdestvenskaya IV, Kogure T, Abe E, Drits VA (2009) A structural model for charoite. *Mineral mag* 73:883–890. <https://doi.org/10.1180/minmag.2009.073.2.883>

Rodkin M.V.¹, Punanova S.A.¹, Martynova G.S.² Trace element composition of natural objects. *UDC* 550.4.41

¹Oil and Gas Research Institute Russian Academy of Sciences, Moscow (rodkin@mitp.ru); ²Institute of Geology and Geophysics, Ministry of Science and Education of Azerbaijan

Abstract The paper presents the results of geochemical studies of the products of activity of mud volcanoes and of oil deposits on the western side of the South Caspian depression. The trace elements (TE), hydrocarbon and component compositions of naphthides from the Absheron, Shamakhi-Gobustan and Nizhnekura regions of Azerbaijan have been examined. Comparison of the TE contents in oils and in oil mud volcanic fluids, as well as isotopic characteristics and biomarkers indicates a common genesis

of the mentioned naphthides. It is noted that in the studied regions, the concentrations of TEs in oil manifestations from mud volcanoes are significantly higher than, on average, in oils of adjacent regions. This feature can be connected with processes of hypergene transformation of oils from seeps from mud volcanoes, loss, volatilization of light fractions, oxidation and biodegradation processes causing the corresponding increase in resinous-asphaltene components and the TE content and in biomarker indicators. The compositions of carbon dioxide and mud volcanic fluids of the Greater Caucasus region, mud volcanic waters of Eastern Georgia, and the Taman Peninsula were analyzed previously also. Based on the correlation coefficients of fluid compositions in the Caucasus region with the compositions of the Earth's crust at different levels, it is shown that the roots of the corresponding deep fluid flows are associated with the Middle Earth's crust. The trends in the metallogeny of hydrocarbon deposits appear to be connected with the tectonic activity of the region and with character of the thermal regime; they confirm the polygenic nature of the sources of trace elements in naphthides.

Keywords: correlation analysis; mud volcanic waters; carbonated waters; hydrocarbon reservoirs; trace elements composition; polygenicity; earth's crust; biota.

Introduction. Modern instrumental methods (trace element, hydrocarbon and component analyzes) have been used to study the composition of products released from mud volcanoes in the form of oil shows in the Apsheron, Shamakhi-Gobustan and Nizhnekura regions of Azerbaijan, as well as oil from the fields of the same regions to establish the genetic commonality of their ontogenesis. The microelement composition (Mn, As, Co, Cr, Mo, Ti, Cu, Li, Ni, Pb, V, Zn, Fe) of naphthides was studied by inductively coupled plasma mass spectrometry (ICP/MS) on a NexION-300 D device from the company "Perkin Elmer" (Punanova et al., 2023). The correlation dependences of the composition of mud volcanic waters and clays of Azerbaijan, the Taman Peninsula and Eastern Georgia with the composition of the Earth's crust were previously studied (Rodkin, Punanova, 2023). As reference models for comparison, we used the models of the chemical composition of the different levels of the Earth's crust (the Upper, Middle and the Lower) according to (Rudnick, Gao, 2003) and models of the chemical composition of biota, with detail into 4 types - marine and terrestrial organisms, plants and animals (Bowen, 1966).

Results and Discussion. Based on the data obtained, the concentration series of trace elements in oil shows of mud volcanoes is presented: $Fe > Ti > Ni > Cr > Mn > Zn > Li > V > Cu > Co > Mo > Pb > As$. All samples are of the ferruginous type, followed by Fe in quantitative content by Ti and Ni. The element contents are quite high, reaching maximum values for Fe, Ti and Ni, respectively, >5000, 190 and 172 ppm. Ni, as a rule, predominates over V

($V/Ni < 1$), and the V concentration amounts to 51 g/t. The results of a comparative analysis of the TE compositions of mud volcanic oil seeps and from oils and gas fields in the same are presented in Fig. 1; the contents of Ni, V, Ti, Zn, Cr and Fe in samples from three regions: Absheron, Shamakhi-Gobustan and Nizhnekura are compared. Comparison of TE contents in samples of oils and oils from mud volcanoes indicates a generally uniform concentration distribution of metals in mud volcanic oils and oil fields of the same regions, with higher concentrations of elements in mud volcanic oils compared to oils from HC fields in the same areas, as well as a significant predominance of Ni above V. Thus, the concentration of V in oil manifestations of volcanic activity varies from 17.2 to 51.8, and Ni from 115 to 137 g/t (averaged data); in field oils these contents are noticeably lower and vary for V from 1.0 to 8.4, and Ni from 9.0 to 13.2 g/t. In accordance with these values, the Ni/V ratios also change (from 6.7 to 2.7, and from 9.0 to 1.5, respectively). The TE analysis of the composition of Azerbaijani oils using a wider database (about 40 elements) is consistent with the presented results. The iron-nickel specificity of the oils of the South Caspian oil and gas basin has also been revealed, the content of Fe and Ni in which prevails over the content of vanadium ($V/Ni < 1$, $V/Fe < 1$) (Babaev, Punanova, 2014; Martynova et al., 2022).

In the South Caspian depression there is a close connection between the distribution of mud volcanism and the oil and gas fields. Mud volcanoes are considered to be modern, actively forming petroleum bearing structures. They are usually confined to zones of tectonic disturbances. From the orogenic elements surrounding the depression to its internal parts, there is a sharp subsidence of the Mesozoic surface and, accordingly, an increase in the thickness of the Cenozoic, the base of which reaches 8-12 km on the Absheron Peninsula, 8-10 km in the Shamakhi-Gobustan and Nizhnekura regions and even 14-20 km on Absheron threshold and in the Southern Caspian Sea. On the western side of the South Caspian depression, on the territory of Azerbaijan, more than 80% of known oil and gas fields are complicated by mud volcanoes. It is noted that the roots of mud volcanoes are confined to deep-seated horizons of the sedimentary section of the South Caspian basin, which are characterized by ultra-high reservoir pressures (80-100 MPa or more). Detailed pyrolytic studies using the Rock-Eval installation of rock samples from mud volcanoes of Azerbaijan, as well as micro-oil in emissions of mud volcanoes, confirmed the possibility of oil and gas formation processes occurring at great depths at high pressures and temperatures (Guliyev et al., 2017; Yusubov, Guliyev, 2022 and etc.).

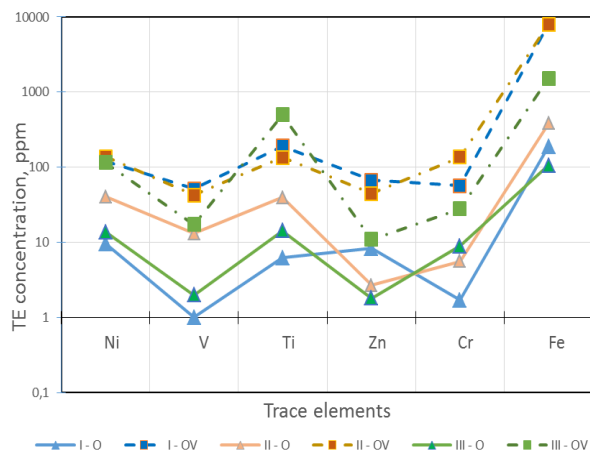


Fig. 1. Assessment of the content of trace elements in oils (O) and oil shows of mud volcanoes (OV) in various regions of Azerbaijan: Absheron (I), Shamakhi-Gobustan (II) and Nizhnekura (III)

Previously, the authors showed that based on the results of the analysis of the waters and clay fraction of the mud volcanoes of Taman and Eastern Georgia and the mud volcanic waters of Azerbaijan, both common features of their composition were identified, which are also characteristic of the composition of carbon dioxide waters of the meganticlinorium of the Greater Caucasus, and differences from carbon dioxide hydrotherms (Rodkin, Punanova, 2023). For both naphthides and carbon dioxide sources, the greatest correlation is observed with the composition of the middle continental crust. At the same time, a very high and almost identical correlation with the compositions of the Upper and Middle crust and a noticeably weaker correlation with the composition of the Lower crust was revealed for clays. For the waters of mud volcanoes, the correlation coefficients are noticeably lower than for clays and carbon dioxide hydrotherms, but the tendency for a maximum correlation with the composition of the Middle crust remains. The maximum correlation with the chemical composition of the Middle crust characterizes the depth of roots of the corresponding fluid systems. For hydrotherms of the Greater Caucasus, this depth corresponds to the depth of the main magmatic chambers, for mud volcanoes - to the depth of the roots of the volcanic structures. At the same time, for the mud volcanoes of Taman, Azerbaijan and Georgia, in contrast to the carbonated waters of the highlands of the Greater Caucasus, the greatest correlation is systematically observed with the chemical composition of not terrestrial, but marine plants and animals (Table 1).

Previously, the authors showed that based on the results of the analysis of the waters and clay fraction of the mud volcanoes of Taman and Eastern Georgia and the mud volcanic waters of Azerbaijan, both

common features of their composition were identified, which are also characteristic of the composition of carbon dioxide waters of the meganticlinorium of the Greater Caucasus, and differences from carbon dioxide hydrotherms (Rodkin, Punanova, 2023). For both naphthides and carbon dioxide sources, the greatest correlation is observed with the composition of the Middle continental crust. At the same time, a very high and almost identical correlation with the compositions of the Upper and the Middle crust and a noticeably weaker correlation with the composition of the Lower crust was revealed for clays. For the waters of mud volcanoes, the correlation coefficients are noticeably lower than for clays and carbon dioxide hydrotherms, but the tendency for a maximum correlation with the composition of the Middle crust remains. The maximum correlation with the chemical composition of the Middle crust characterizes the depth of occurrence of the corresponding fluid flows. For hydrotherms of the Greater Caucasus, this depth corresponds to the depth of the main magmatic chambers, for mud volcanoes - to the depth of the roots of these volcanoes. At the same time, for the mud volcanoes of Taman, Azerbaijan and Georgia, in contrast to the carbonated waters of the highlands of the Greater Caucasus, the greatest correlation is systematically observed with the chemical composition of not terrestrial, but marine plants and animals (Table 1).

The results of calculations of correlation coefficients between the TE content of mud volcanic waters of Azerbaijan (according to analytical data (Lavrushin et al., 2015)) with the model composition of the continental crust and biota - marine and terrestrial (previously obtained in combination with the TE composition of carbon dioxide waters of the Greater Caucasus) indicate the prospects deep sediments of the South Caspian oil and gas basin. The highest correlation of the TE composition of mud volcanic waters in Azerbaijan (all three studied regions) is noted with the composition of the Middle crust compared to the compositions of the Upper and the Lower crust. There is also a higher correlation with the chemical composition of marine fauna rather than terrestrial fauna. This is an indication of the sapropel-humus type of the initial OM, which is consistent with the geochemical characteristics of HC generation processes in the basin.

Let us emphasize the hypothetical point for now that the results of the correlation analysis of the TE composition of objects, namely a high connection with the composition of the Middle crust, indicate a fairly deep origin of water in the mud volcanoes of Azerbaijan, which is consistent with seismological data (Sobisevich et al., 2008; Shnyukov, Netrebskaya, 2013) about the large, up to 15-20 km,

depth of the roots of a few mud volcanoes of the Black Sea and Azerbaijan and with data on the typical depths of the main magma chambers of the volcanoes (here, Elbrus and Kazbek).

Table 1. Correlation coefficients between the compositions of water, crust and biota

Region (number of tests)	Earth crust			Biota			
	Upper	Middle	Lower	Marine		Terrestrial	
				plants	animals	plants	animals
Absheron (5)	0.42±0,04	0.48±0,04	0.44±0,04	0.72±0,04	0.77±0,02	0.67±0,02	0.65±0,03
Shemakha-Gobustan (23)	0.42±0,01	0.48±0,01	0.44±0,01	0.75±0,01	0.76±0,01	0.66±0,01	0.67±0,01
Kura river (12)	0.47±0,03	0.55±0,03	0.50±0,03	0.76±0,02	0.79±0,01	0.70±0,01	0.69±0,01

Note: the error in estimating the average correlation coefficient is given; the maximum correlation values (for the crust and biota) are highlighted in bold.

Conclusion

Geochemical study of the composition of the products of mud volcanism emissions and oils on the western side of the South Caspian Basin makes it possible to clarify the nature of the deep horizons of the Earth's crust as probable sources of hydrocarbons, to clarify the nature of the ontogenesis of hydrocarbon accumulations and, ultimately, contributes to a better assessment of the prospects for searching for oil and gas accumulations on large depths. The revealed relationship between the correlation coefficients of the TE composition of the waters of the mud volcanoes of Azerbaijan and the composition of the Middle crust may indicate the involvement of deeper horizons in the processes of oil and gas formation, and a possible additional source of TE. The polygenic nature of the TE composition of oils has been repeatedly indicated in many publications. Involving a wide range of TEs (rare earth elements, platinum group metals, radioactive elements) in the study will help solve controversial problems more substantively.

Financing. The work was carried out within the framework of the budget plans of the Institute of Oil and Gas Engineering of the Russian Academy of Sciences (topics “Scientific and methodological foundations for searching and exploration of oil and gas accumulations confined to mega-reservoirs of the sedimentary cover”, No. 1220222800253-3, “Fundamental basis of energy-efficient, resource-saving and environmentally friendly, innovative and digital search technologies, exploration and development of oil and gas fields, research, production and development of traditional and unconventional reserves and resources of oil and gas; development of recommendations for the sale of oil and gas complex products in the context of the energy transition and EU policy on energy decarbonization (fundamental, exploratory, applied, economic and interdisciplinary). research”, No.

122022800270-0 and the thematic plan of the IGG of the Ministry of Science and Education of the Republic of Azerbaijan (topic “Fluid dynamics of the convergence zone of the Black Sea-Caspian segment of the Eurasian and Arabian plates”).

References

- Babaev F.R., Punanova S.A. Geochemical aspects of the microelement composition of oils. Scientifically edited by Academician of ANAS I.S. Gulieva. M.: Nedra Publishing House LLC, 2014. 181 p.
- Guliev I.S., Kerimov V.Yu., Osipov A.V., Mustaev R.N. Generation and accumulation of hydrocarbons in conditions of great depths of the earth's crust // SOCAR Proceedings. 2017. No. 1, 004-0016.
- Lavrushin V.Yu., Guliev I.S., Kikvadze O.E., Aliev A.A., Pokrovsky B.G., Polyak B.G. Waters of mud volcanoes of Azerbaijan: isotope-geochemical features and formation conditions // Lithology and minerals. 2015. No. 1. P. 3-29.
- Martynova G.S., Nanadzhanova R.G., Guliev I.S. Patterns of distribution of microelements in oil manifestations of mud volcanoes // East European Scientific Journal. 2022. 2(78). P. 21-26.
- Punanova S.A., Guseinov D.A., Martynova G.S., Nanajanova R.G. Geochemical features of oils and oil manifestations of mud volcanoes on the western side of the South Caspian depression // Geology of oil and gas. 2023. No. 6. P. 97-106. DOI: 10.47148/0016-7894-2023-6-97-106
- Rodkin M.V., Punanova S.A. Correlation dependencies of the microelement composition of natural objects // Geology of oil and gas. 2022. No. 4. P. 99-107.
- Yusubov N.P., Guliev I.S. Mud volcanism and hydrocarbon systems of the South Caspian basin (according to the latest data from geophysical and geochemical studies). Baku, Elm, 2022, 168 p.
- Bowen H.J. Trace elements in biochemistry. London, New York: Acad. press, 1966. 241 p.
- Rudnick R.L., Gao S. Composition of the continental crust // Elsevier. 2003. No. 3. P. 1-64.

Rodkin M.V.^{1,2}, Punanova S.A.², Rukavishnikova T.A.¹ On the nature of the relationship of the trace elements composition of deep fluids with the chemical composition of the Upper, Middle and the Lower crust and biota. UDC 550.8:622.276

¹Institute of Earthquake Prediction Theory and Mathematical Geophysics, Russian Academy of Sciences, Moscow; ²Oil and Gas Research Institute Russian Academy of Sciences, Moscow (rodkin@mitp.ru)

Abstract A database of more than 300 analyzes of the trace elements (TE) composition of caustobioliths and hydrocarbons, mud volcanic, and carbonic fluids with the determination of a large number of elements has been compiled. The correlation coefficients of the concentration logarithms were calculated, which makes it possible to take into account data on elements with both high and very low concentration. For the analyzed oils the correlation between the TE composition and the composition of the Lower crust is found to be strongest. The results are interpreted as an indication of the role of the deep fluids (from the level of the Lower crust) in the processes of oil genesis and as another evidence of the implementation of uprising deep fluid flows in the Earth's crust, the existence of which was also revealed by seismological data.

Keywords: trace elements; deep fluids; correlation analysis; compositions of the Earth's crust and biota.

Introduction and Data. Analysis of the trace element (TE) composition of various fluids is a well-known research method. However, there has been no previous systematic attempt to compare the TE composition of various deep fluids with the chemical composition of the main georeservoirs: the Upper, Middle and Lower crust and different types of biota (plants and animals, aquatic and terrestrial). To compile a database (DB) on the TE composition of deep fluids, literature data from various authors was used. Taking into account the specifics of further processing, only the results of analyzes with the determination of a large (at least 30) number of elements were taken into account; preference was given to more recent works. A significant part of the database characterizes the TE composition of hydrocarbon fluids: crude oils, oil fractions and oil degradation products (Gottikh et al., 2007; 2009; Maslov et al., 2010; Varfolomeev et al., 2011; Dobretsov et al., 2015; Mikhailova, 2021; Ivanov et al., 2022; etc.). In addition to determinations of the TE composition of Eurasian naphthides, the DB presents world data, as well as, in more detail, data on the TE composition of crude oils from California and Trinidad (Yang Weihang, 2014; 2019; Yang Weihang et al, 2018). Also presented are data on the TE composition of carbon-containing formations of supposedly source rocks (mainly based on data for the West Siberian and Volga-Ural oil and gas basins (OGB)). The results of the TE composition of mud

volcanic waters and mud volcanic breccia are presented with data for the Caucasus region (basins of the Black, Caspian and Azov seas). In addition to hydrocarbon fluids, the database contains TE data on the composition of carbon dioxide and partly hydrothermal waters of the Greater Caucasus (Lavrushin, 2012). In total, the database includes more than 300 test results. In general, the database makes it possible to fairly confidently characterize the main features of the TE composition of deep fluids, represented by both reduced (hydrocarbon, mud volcanic) and oxidized (carbon dioxide) components.

Models of the chemical composition of the main different-depth levels of the continental crust and the chemical content of living organisms were used as reference models for comparison. Namely, for the correlation analysis of TE compositions of deep fluids, refined models of the chemical composition of different levels of the Earth's crust (the Upper, Middle and Lower) according to the data of (Rudnick, Gao, 2003) and models of the chemical composition of biota, with detail on marine and terrestrial plants and animals (Bowen, 1966; Kowalski, 1970).

When presenting data on TE analysis, the option of presenting concentration values on a logarithmic scale is quite often used. But as far as the authors know, calculations of correlations with different horizons of the Earth's crust and with different types of biota have not been previously carried out. In such calculations, the concentration values were represented by logarithms of concentration. The reason for the transition to logarithms is that this allows calculations to take into account data on the concentration of elements with very low content; on a conventional linear scale these concentrations would be indistinguishable from zero and would effectively be ignored. Correlation calculations were carried out for the entire data set of the database described above.

Results and Discussion. Typical calculation results for the TE composition of naphthides and carbon-containing matter in rocks are presented in Table. 1 (Rodkin et al., 2016; Punanova, Rodkin, 2019; Rodkin, Punanova, 2023, etc.).

In the cases presented in the table, a general pattern is observed, presented in the previous works of the authors (Rodkin et al., 2016; and others). For rock types that are obviously near-surface in their genesis (clays, coals, shales), the maximum correlation is expectedly observed with the chemical composition of the Upper crust. For biota, there is a stronger association with marine plants, indicating that the dominant source of organic matter was marine plants (usually dominant in mass in sedimentary basins). For the TE composition of the

oils considered, the situation in the overwhelming majority of cases is different. The correlation is stronger with the Lower crust than with the Upper crust. At the same time, the connection with the biota and the increase in connection with the Lower crust compared to the Upper crust grows in sequence from

the carbon-containing host rocks to oils and to oil degradation products (asphalts). The exception is oil and oil occurrences in Kamchatka, for which the connection with the Middle or Upper crust is stronger.

Table 1. Average values of correlation coefficients for naphthides; typical examples

Object, location	Earth crust			Biota			
	Upper	Middle	Lower	Aquatic plants	Terrestrial plants	Aquatic animals	Terrestrial animals
Coins, shale, clays (Shpirt, Punanova, 2010)							
Coins	0.84	0.76	0.77	0.78	0.71	0.48	0.50
Oil shale	0.84	0.76	0.79	0.76	0.74	0.54	0.55
Black shale	0.82	0.83	0.80	0.78	0.75	0.57	0.56
Clays	0.90	0.85	0.83	0.77	0.72	0.53	0.46
Average	0.85±0.02	0.80±0.03	0.80±0.01	0.77±0.01	0.73±0.01	0.53±0.02	0.52±0.02
Bitumen, bitumoids, asphalts (Gottikh et al., 2007, 2008)							
Bitumen	0.74±0.05	0.69±0.05	0.73±0.05	0.69±0.02	0.48±0.05	0.49±0.05	0.38±0.05
Bitumoids	0.65±0.05	0.63±0.05	0.66±0.04	0.66±0.04	0.69±0.03	0.62±	0.56±0.03
Asphalts, host rocks (Mikhailova, 2021)							
Asphalts	0.47±0.02	0.50±0.02	0.50±0.02	0.31±0.03	0.50±0.03	0.49±0.02	0.43±0.02
Domanic rocks	0.79±0.03	0.79±0.03	0.79±0.03	0.71±0.02	0.66±0.01	0.61±0.01	0.57±0.01
Oils (Gottikh et al., 2016)							
Timan-Pechora	0.66±0.02	0.66±0.02	0.72±0.0.02	0.60±0.02	0.63±0.02	0.59±0.02	0.54±0.01
Oils (Veshev et al., 2000)							
Baltic region	0.51±0.02	0.51±0.02	0.57±0.02	0.60±0.5	0.53±0.05	0.29±0.03	0.39±0.03
Oils (Maslov et al., 2010)							
Udmurtia	0.70±0.01	0.69±0.01	0.74±0.01	0.41±0.01	0.61±0.01	0.53±0.01	0.55±0.01

For the case of carbonated waters of the Greater Caucasus, the correlation with the composition of the Lower crust turns out to be significantly lower than with the Middle and the Upper crust; Moreover, the connection with the Middle crust is slightly higher than with the Upper crust. The composition of the biota is most closely related to terrestrial plants, which is in good agreement with the topography and geological history of the Greater Caucasus. For mud volcanic waters in the basins of the Black and Caspian Seas, the connection with the composition of the Middle crust and with aquatic organisms is maximum.

Conclusions. The vast majority of oils are characterized by lower correlations between their trace element composition and biota and higher correlations with the chemical composition of the Lower crust. This trend is interpreted as a reflection of the transformation of organic matter of sedimentary strata under the influence of the ascending flow of lower crustal (possibly deeper) fluids in accordance with the model of oil genesis

according to the scheme of a flow-through nonequilibrium reactor (Rodkin, Rukavishnikova, 2015; Punanova, Rodkin, 2019). The specific TE composition of Kamchatka oils is explained by higher crust temperatures, at which dehydration reactions occur at shallower depths, and the ascending fluid flow carries mark of a shallower level. The presence of upward flows of deep fluid is strongly supported by the analysis of seismological data, as well as the difference in the nature of seismic-ionospheric connections in earthquakes of different depths (Rodkin, 2022; Rodkin, Liperovskaya 2023). Taken together, these data make it possible to more fully characterize the main features of the deep fluid regime of the lithosphere.

Financing. The work was carried out within the framework of the budget plan of the Institute of Oil and Gas Engineering of the Russian Academy of Sciences (themes “Scientific and methodological foundations for searching and exploration of oil and gas accumulations confined to mega-reservoirs of the sedimentary cover”, No. 122022800253-3, “Fundamental basis of energy-

efficient, resource-saving and environmentally friendly, innovative and digital search technologies, exploration and development of oil and gas fields, research, production and development of traditional and unconventional reserves and resources of oil and gas; development of recommendations for the sale of oil and gas complex products in the context of the energy transition and EU policy on energy decarbonization (fundamental, exploratory, applied, economic and interdisciplinary). research)", No. 122022800270-0).

References:

- Varfolomeev S.D., Karpov G.A., Sinal G.A., Lomakin S.M., Nikolaev E.N. The youngest oil on Earth // *Dokl. Academy of Sciences*. 2011. T. 438, no. 3. P. 345–347.
- Vinogradov A.P. *Biogeochemistry* // TSB. Ed. 3rd. T. 3. M.: Soviet Encyclopedia, 1970. P. 329–330.
- Gottikh R.P., Pisotsky B.I., Zhuravlev D.Z. The role of endogenous fluids in the formation of carbon-containing rocks in the geological section of oil and gas provinces // *Dokl. Academy of Sciences*. 2007. T. 412, No. 4. P. 524–529.
- Gottikh R.P., Lukin A.E., Pisotsky B.I. Geochemical aspects of the formation of carbonaceous substances in the Dnieper graben and the south of the Siberian platform // *Dokl. Academy of Sciences*. 2008. T. 419, No. 5. P. 665–669.
- Gottikh R.P., Vinokurov S.F., Pisotsky B.I. Rare earth elements as geochemical criteria for endogenous sources of trace elements in oil // *Dokl. Academy of Sciences*. 2009. T. 425, No. 2. P. 223–227.
- Gottikh R.P., Pisotsky B.I., Malinina S.S., Chernenkova A.I. The role of deep processes in the formation of hydrocarbon accumulations in the Timan-Pechora oil and gas province // *Geology of oil and gas*. 2016. No. 3. P. 86–101.
- Dobretsov N.L., Lazareva E.V., Zhmodik S.M. and others. Geological, hydrogeochemical and microbiological features of the oil site of the Uzon caldera (Kamchatka) // *Geology and Geophysics*. 2015. T. 56, No. 1–2. P. 56–88.
<https://doi.org/10.15372/GiG20150103>
- Lavrushin V.Yu. *Underground fluids of the Greater Caucasus and its surroundings*. M.: GEOS, 2012. 348 p. DOI:10.13140/2.1.2775.0088.
- Maslov A.V., Ponomareva S.A., Ronkin Yu.L. REE systematics of crude oils from the Karsovaiskoye field (Republic of Udmurtia). Ekaterinburg: UrGGU, 2010. P. 242–253.
- Mikhailova A.N. The influence of hydrothermal effects on the efficiency of hydrocarbon extraction from high-carbon Domanik rocks. Diss. ... Ph.D. Kazan, 2021. 148 p.
- Punanova S.A., Rodkin M.V. Comparison of the contribution of geological processes at different depths to the formation of the microelement appearance of caustobiolites // *Georesursy*. 2019. T. 21. No. 3. P. 14–24. DOI: <https://doi.org/10.18599/grs.2019.3.14-24>.
- Rodkin M.V., Rukavishnikova T.A. The source of oil formation as a nonequilibrium dynamic system - a model and comparison with empirical data // *Geology of oil and gas*. 2015. No. 3. P. 63–68.
- Rodkin M.V., Rundqvist D.V., Punanova S.A. On the relative role of lower-crustal and upper-crustal processes in the formation of the microelement composition of oils // *Geochemistry*. 2016. No. 11. P. 1025–1031.
- Rodkin M.V., Liperovskaya E.V. On the differences in the physical mechanisms of earthquakes at different depths and the nature of their ionospheric response // *Physics of the Earth*. 2023. No. 3. P. 48–62.
- Taylor S.R., McLennan S.M. *Continental crust: its composition and evolution*. M.: Mir, 1988. 384 p.
- Shpirt M.Ya., Punanova S.A. Features of the microelement composition of coals, shale and oils of various sedimentary basins // *Chemistry of solid fuels*. 2010. No. 4. P. 57–65.
- Bowen H.J. *Trace elements in biochemistry*. London; New York: Academic Press, 1966. 241 p.
- Ivanov K.S., Erokhin Y.V., Kudryavtsev D.A. Inorganic geochemistry of crude oils of Northern Eurasia after ICP-MS data as clear evidence for their deep origin // *Energies*. 2022. V. 15, Iss. 1. Art. 48.
<https://doi.org/10.3390/en15010048>
- Rodkin M.V., Ngo Thi Lu, Punanova S.A. Correlation of trace element composition of oils and other caustobiolites with chemical content of different types of biota and the Upper, Middle and the Lower Earth's Crust // *Vietnam Journal of Earth Sciences*. 2021. V. 43. No. 1. P. 23–31. <http://doi.org/10.15625/0866-7187/15573>.
- Rodkin M.V. The Variability of Earthquake Parameters with the Depth: Evidence of Difference of Mechanisms of Generation of the Shallow, Intermediate-Depth, and the Deep Earthquakes // *Pure Appl. Geophys*. 2022. <https://doi.org/10.1007/s00024-021-02927-4>
- Rodkin M.V., Punanova S.A. Correlation Analysis of Trace Element Content in Caustobiolites: The Deep Fluid Involvement, Conjunction of Features of Organic and Inorganic Models of Oil Genesis // *Progress Petrochem Sci*. 2023. 5(2). P.P.S. 000608. DOI: 10.31031/PPS.2023.05.000608
- Rudnick R.L., Gao S. *Composition of the continental crust* // *Treatise on Geochemistry*. 2003. V. 3. P. 1–64.
<https://doi.org/10.1016/B0-08-043751-6/03016-4>
- Yang Weihang. High Precision Determination of Trace Elements in Crude Oils by Using Inductively Coupled Plasma-Optical Emission Spectrometry and Inductively Coupled Plasma-Mass Spectrometry. PhD diss., 2014.
- Yang, Weihang A. Method for High Precision Determination of Up to 57 Trace and Ultra-Trace Elements in Crude Oils Using Triple Quad-ICP-MS with Applications in Exploration, Production Allocation and Refining. 2019. University of Houston <https://hdl.handle.net/10657/5850>. Doctoral Thesis.
- Yang W., Gao Y., Casey J. F. Determination of trace elements in crude oils and fuel oils: A comprehensive review and new data. In: Xiong Y (Ed.), *Solution chemistry: Advances in research and applications*, Hauppauge, Nova Science Publishers, New York, 2018. USA. P. 159–205.